ECS Solid State Letters, **1** (2) P22-P25 (2012)
2162-8742/2012/1(2)/P22/4/$28.00 © The Electrochemical Society

The Effect of Al and Ni Top Electrodes in Resistive Switching Behaviors of Yb_2O_3-Based Memory Cells

Somnath Mondal,[a] Jim-Long Her,[b] Fu-Hsiang Ko,[c] and Tung-Ming Pan[a,z]

[a]*Department of Electronics Engineering, Chang Gung University, Taoyuan 333, Taiwan*
[b]*Division of Natural Science, Center for General Education, Chang Gung University, Taoyuan 333, Taiwan*
[c]*Department of Materials Science and Engineering, Institute of Biological Science and Technology, National Chiao-Tung University, Hsinchu 300, Taiwan*

In this letter, the effect of Al and Ni top electrodes in resistive switching behavior of Al/Yb_2O_3/TaN and Ni/Yb_2O_3/TaN memory devices is proposed. The Al/Yb_2O_3/TaN memory device demonstrates no such switching performance as applying bias on both top and bottom electrodes, whereas the Ni/Yb_2O_3/TaN reveals the bipolar memory switching behavior with a high resistance ratio of 10^4 for over 200 cycles of switching responses and good data retention with memory window of about 10^5 at 85°C, as extrapolated up to 10 years. The resistance switching dynamic is ascribed to the conductivity modulation by oxygen ions/vacancies controlled electrochemical reaction process in the Yb_2O_3 switching layer.
 [DOI: 10.1149/2.005202ssl]

Manuscript received April 19, 2012. Published July 20, 2012.

Resistive random access memory (ReRAM) is an emerging storage device for next generation high potential nonvolatile memory (NVM) applications due to its scaling ability, low cost, and compatibility of being integrated in back-end-of-line (BEOL) process in complementary metal-oxide-semiconductor (CMOS) fabrication.[1–7] A simple ReRAM device structure usually consists of an oxide layer sandwiched between two metal electrodes. Application of low voltage electrical pulse with certain level can change the oxide's resistance significantly between two stable states, namely high resistance state (HRS) and low resistance state (LRS). Nonvolatile resistive switching behavior has been demonstrated for several binary oxides, including TiO_2, Ta_2O_5, Al_2O_3, ZrO_2, and Yb_2O_3.[8–13] Although resistance-switching phenomena in several binary metal oxides have been known from decades, the details of the switching mechanisms and the nature of the different resistive states are still under debate. Different switching models such as domain and tunneling model,[14] filament model,[15,16] and field induced crystallinity and charge trapping model[17–19] have been studied extensively. However, exact switching phenomena are not clearly understood yet. In this letter, we explored an improved resistive switching behavior of Ni/Yb_2O_3/TaN memory cells in compare with Pt/Yb_2O_3/TiN memory cell.[13] Additionally, the influence of top electrode material (Ni and Al) on the electrical properties of Yb_2O_3-based ReRAM is discussed to realize for next generation universal memory application.

It is found that the bipolar resistive switching behavior in Ni/Yb_2O_3/TaN ReRAM cell keeps stable resistance ratio of 10^4 with switching responses over 200 cycles. Good data retention for 10^5 s with sufficient memory window at 85°C is also demonstrated. The resistance switching dynamic is attributed to the filamentary conduction of oxygen ions/vacancies by electrochemical reaction process in the Yb_2O_3 switching layer.

Experimental

The TaN bottom electrode was deposited on SiO_2/Si substrates by sputter deposition technique. Then, a 30-nm Yb_2O_3 thin film was deposited on the TaN by radio frequency (rf) magnetron sputtering with an Ar/O_2 atmosphere using a metallic Yb target. The chamber working pressure was maintained at 10^{-2} Torr, while the Ar/O_2 flow was set at 3:1 proportion. A shadow mask with circular areas (100 μm diameter) was used to define the top electrode. Finally, a 100-nm top electrode (Al or Ni) was deposited by means of thermal evaporation technique. The merits of Ni electrode are low cost, high work function and compatibility with existing CMOS process. X-ray diffraction (XRD) and X-ray photoelectron spectroscopy (XPS) were employed to determine the structure and the chemical bonding state of the Yb_2O_3 thin films, respectively. The electrical measurements were performed in dark with Agilent E5260A high speed semiconductor parameter analyzer. The bottom electrode TaN was grounded and the signals were applied to the top electrode in all the measurements.

Results and Discussion

Fig. 1a shows the XRD micrograph of as-deposited Yb_2O_3 thin film grown on TaN bottom electrode. Presence of no Yb_2O_3 peak in the data revealed an amorphous phase of the film, whereas the previous result showed some nanocrystal in the oxide film.[13] This may be due to different deposition conditions in sputtering system. Inset of Fig. 1a shows cross sectional TEM image of the Yb_2O_3 thin film, corroborates well with the XRD data. The core level O 1s spectra with their appropriate peak curve-fitting lines for the Yb_2O_3 film are shown in Fig. 1b. The O 1*s* spectrum at the surface of Yb_2O_3 thin film consists of a low peak binding energy at 529.4 eV for Yb_2O_3 lattice oxygen ions, and a high peak binding energy at 531.9 eV indicates a large amount of non-lattice oxygen ions usually attributed to OH^- groups. Rare-earth oxide is known to actively react with OH due to its hydration characteristics.[20]

Fig. 2a shows the current-voltage (I-V) characteristics of the fabricated Al/Yb_2O_3/TaN ReRAM cell before and after electro-forming process. The memory device using Al top electrode exhibited no switching characteristics after electroforming process. This can be attributed to the formation of stable Al-O layers at the Al and Yb_2O_3 interface due to the lower workfunction and higher oxygen affinity of Al electrode.[21] By applying voltage stress on either polarity at the Al electrode, an irreversible switching occurs which is commonly depicted as hard breakdown of dielectric. Furthermore, to look at the electrode thickness dependence resistive switching behavior, the Al/Yb_2O_3/TaN memory device with different Al thicknesses was investigated. All devices with an Al top electrode show no resistive switching characteristics in this study. In contrast, the ReRAM cell with Ni top electrode exhibit a reproducible bipolar resistive switching behavior by dc double sweep for more than 200 sweeping cycles, as depicted in Fig. 2b. An electrical forming process is required to initiate the switching process by dc negative voltage sweeping with a compliance current of 0.1 mA. After the forming process, the device switches to LRS. By sweeping the voltage to opposite polarity above reset value (V_{reset}) of about 2 V, a sudden decrease in conduction current is observed. The resistance of the memory cell switches from LRS to HRS. Contrariwise, the cell turns back to LRS while applying a negative bias over set voltage (V_{set}) about −2.5 V. A current compliance of 1 mA was assigned to prevent the permanent breakdown of the memory devices during switching process. We consider that, the

[z]E-mail: tmpan@mail.cgu.edu.tw

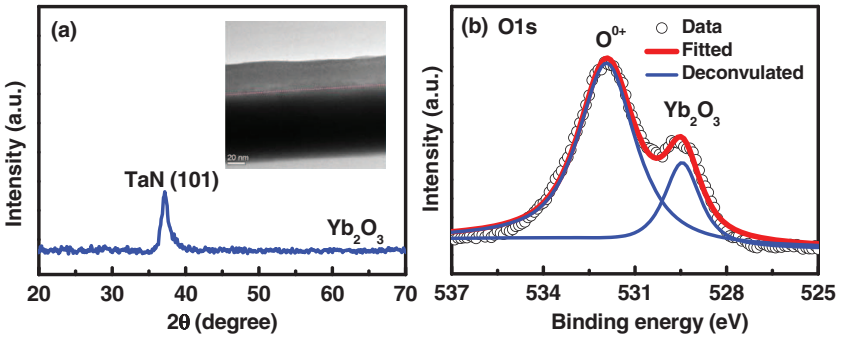

Figure 1. (a) XRD micrograph of Yb_2O_3 thin film deposited on TaN electrode. The inset shows the cross sectional TEM image of the Yb_2O_3 film. (b) the corelevel O1s spectrum on the surface of Yb_2O_3 thin film.

high work-function metal electrode with low oxygen affinity as anode and high oxygen gettering electrode as cathode facilitate to produce stable resistive switching characteristics in Ni/Yb_2O_3/TaN memory device.[13,22]

To clarify the origin of a bipolar resistive switching behavior, the current conduction mechanism of HRS and LRS was investigated. The I-V curves were plotted on the logarithmic scale, as shown in Fig. 3a. In the HRS, the I-V characteristics of a Ni/Yb_2O_3/TaN device show linear behavior up to approximately 0.1 V, suggesting that the thermionic emission limited conduction (TELC) is the dominant mechanism at the lower regime, where carrier injection from the electrode plays a minor role. Beyond that, the increase in the slope is observed, as determined by the fit $I \propto V^n$ ($n = 2$ and 3), which can be understood as a transition of conduction mechanism from Ohmic TELC to space charge limited current (SCLC). In the LRS, the slope is nearly constant as 1, which represents that the Ohmic conduction is dominant in all bias range during LRS. This may be due to the filamentary conduction of the accumulated oxygen vacancies into the oxide.[23] Fig. 3b presents the resistances of the LRS and the HRS as a function of temperature. In HRS, the resistance value decreases as the temperature increase from 300 K to about 400 K and this can be associated with a semiconducting behavior of the oxide film while, the resistance at LRS increases as the temperature rises, which indicates weak metallic like behavior. As a consequence, the resistance ratio decreases about one order over a temperature range of 300 - 400 K. This can be attributed to the built-up of oxygen vacancy related traps inside the Yb_2O_3 film.[24]

Based on the above observation, we proposed the switching mechanism in the Ni/Yb_2O_3/TaN device as the migration of charge particles, most possibly ions. It has been reported that oxygen vacancies in some metal oxides give rise to delocalized conduction electrons rather than localized in the band-gap region[25,26] and, hence, it is assumed that the oxygen vacancies in Yb_2O_3 are ionized and act as mobile space charges. This is confirmed by the presence of large amount of nonlattice oxygen ions in the XPS spectrum in Fig. 1b. It is also believed that the low work function metals have more stable oxide and act as a sink for oxygen creating more oxygen vacancies in the oxide.[27] Therefore, it can be speculated that the physisorption or chemisorption of oxygen ions into the TaN electrode leads to the formation of oxygen vacancies or metallic defects in the Yb_2O_3 layer. The electrochemical reaction with the Kröger-Vink notation is given by

$$O_O^{\times}(Me) + V_O^{\bullet\bullet}(O_{\times}) \leftrightarrow V_O^{\bullet\bullet}(Me) + O_O^{\times}(O_{\times}) \quad (1)$$

where *Me* and O_x in the parentheses represent the metal electrode and oxide, respectively, and oxygen ions are assumed to have a charge of −2. During the forming process at sufficient large electric field, the nonlattice oxygen ions in the Yb_2O_3 film drift toward TaN electrode. The accumulated large number of oxygen vacancies in the oxide/TaN interface modulates the conductivity of the oxide, resulting in the device switched from HRS to LRS. Stressing back by opposite polarity of bias, oxygen ions releasing from the TaN electrode will neutralize oxygen vacancies; hence the bipolar behavior is prompted upon the annihilation of oxygen vacancies.[12,13] Fig. 4 shows the driving mechanism of the resistive memory switching due to the physisorption or chemisorption of oxygen ions near the TaN electrode interface at different bias polarities on the device. Conversely, for positive forming, the electrochemical reaction of Eq. (1) occurs near the top electrode. At the Ni/Yb_2O_3 interface, the electrode is oxidized by oxygen ions and no switching is observed likely in the Al/Yb_2O_3/TaN ReRAM cell.

Fig. 5 shows the dependence of the resistance on the repetitive switching cycles of a Ni/Yb_2O_3/TaN ReRAM cell at both room temperature and 85°C. The device resistance values were read out at 0.2 V, while set and reset were performed at negative and positive voltage sweeping, respectively. It can be seen from the experimental data, the LRS was dispersed in a narrow range around 100 Ω, while the HRS value was somewhat fluctuant in the range around 10 MΩ. The resistance ratio of HRS to LRS was in the range of 4-5 orders of magnitude within the 200 cycles. To compare with other work,[12,13] the Ni/Yb_2O_3/TaN ReRAM cell exhibits a higher memory window for operation. This may be attributed to different conditions of the oxide film in the ReRAM device. Moreover, the uniformity of memory parameters such as resistance values is also a very important parameter for practical application. In the inset of Fig. 5, the statistics of two resistance states at room temperature are depicted. A clear and non overlap window of resistances between HRS and LRS ensured

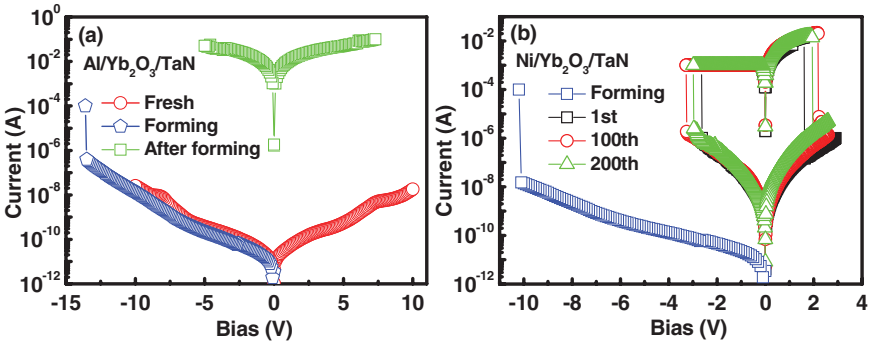

Figure 2. (a) I-V characteristics of Al/Yb_2O_3/TaN ReRAM devices before and after electroforming process. (b) Typical resistive switching characteristics of Ni/Yb_2O_3/TaN ReRAM devices cell after standard electroforming process for 1st, 10th, and 200th sweeping cycles.

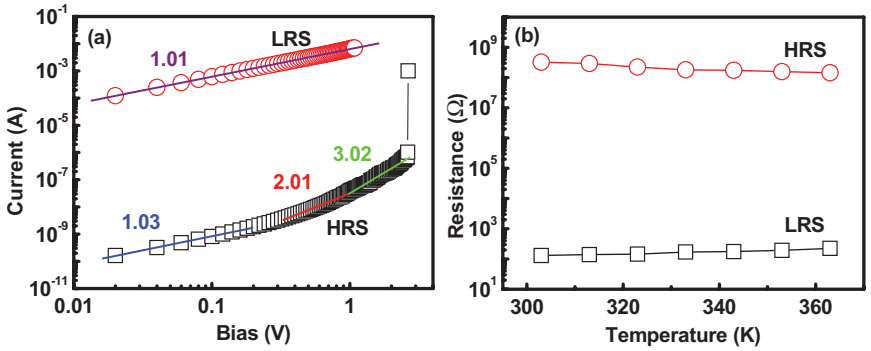

Figure 3. (a) Double logarithmic plots of |I|-|V| curves of Ni/Yb_2O_3/TaN ReRAM device. (b) Temperature dependent resistance values of the memory cell at HRS and LRS.

the Yb_2O_3-based device can be well operated in the application of ReRAM.

To confirm the potentiality in memory application, the data retention properties of the fabricated Ni/Yb_2O_3/TaN ReRAM cell in HRS and LRS were also measured at room temperature (RT) and 85°C, respectively. As shown in Fig. 6, the time-dependent resistance evolution exhibits little change in the magnitude of resistance in HRS, while no significant change of the same in LRS after the duration for 4×10^4 s, and demonstrates extrapolated 10-year retention with nondestructive read-out under both temperatures. The superior data retention characteristics of the Ni/Yb_2O_3/TaN ReRAM cell reveal the potential for nonvolatile memory applications.

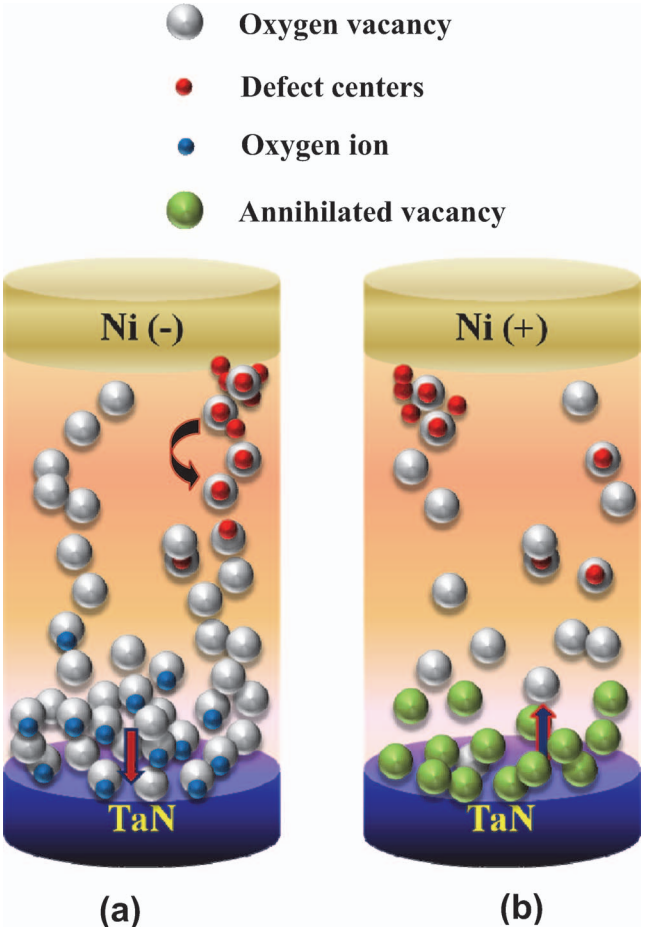

Figure 4. Schematic of driving mechanism of resistive memory switching by filamentary conduction due to physisorption/chemisorption of oxygen ions at TaN electrode.

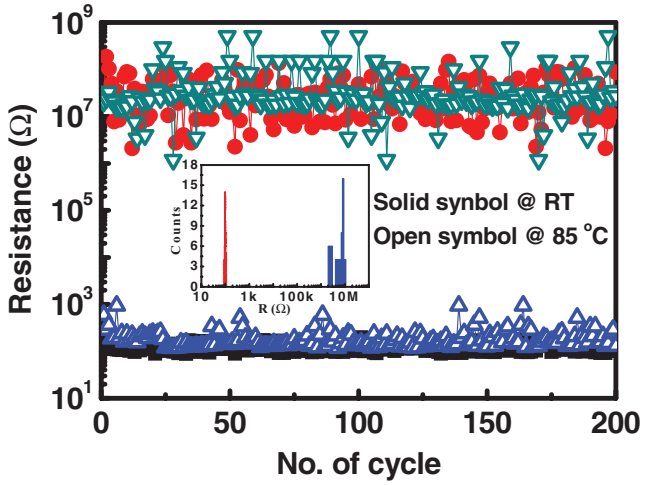

Figure 5. Endurance characteristics of Ni/Yb_2O_3/TaN ReRAM device for DC sweeping cycles at room temperature and 85°C. The inset shows the distribution of resistance values for 200 switching cycles.

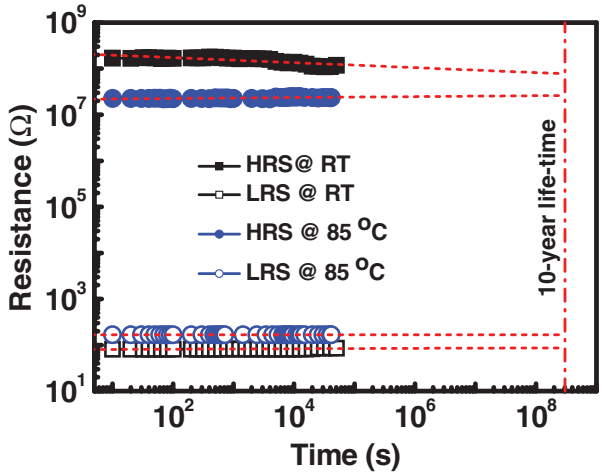

Figure 6. Data retention performance of the Ni/Yb_2O_3/TaN ReRAM device in HRS and LRS under room temperature and 85°C, respectively. The extrapolation method is employed to give a long-term (10-year) prediction result.

Conclusions

In summary, the influence of Al and Ni electrodes in resistive switching characteristics of Al/Yb_2O_3/TaN and Ni/Yb_2O_3/TaN memory devices was investigated for nonvolatile random access memory applications. The switching behavior of Yb_2O_3-based memory cell is related with the properties of the top electrode material. The Ni/Yb_2O_3/TaN ReRAM device exhibited good endurance of over 200 dc switching cycles and nondestructive readout for 10-year data retention performance maintaining the memory window of $\sim 10^5$ at 85°C. The resistive switching in Ni/Yb_2O_3/TaN ReRAM cell could be regarded as the formation/annihilation of conducting filaments in Yb_2O_3 layer by electrochemical reaction process. The Ni/Yb_2O_3/TaN memory cell is very promising candidate for future nonvolatile memory applications.

Acknowledgment

This project was supported by the National Science Council (NSC) of Republic of China under contract no. NSC-97-2221-E-182-050-MY3.

References

1. B. J. Choi, D. S. Jeong, S. K. Kim, C. Rohde, S. Choi, J. H. Oh, H. J. Kim, C. S. Hwang, K. Szot, R. Waser, B. Reichenberg, and S. Tiedke, *J. Appl. Phys.*, **98**, 033715 (2005).
2. H. Akinaga and H Shima, *Proc. IEEE*, **98**, 2237 (2010).
3. K. Szot, W. Speier, R. Carius, U. Zastrow, and W. Beyer, *Phys. Rev. Lett.*, **88**, 75508 (2002).
4. S. Tsui, A. Baikalov, J. Cmaidalka, Y. Y. Sun, Y. Q. Wang, Y. Y. Xue, C. W. Chu, L. Chen, and A. J. Jacobson, *Appl. Phys. Lett.*, **85**, 317 (2004).
5. S. Seo, M. J. Lee, D. H. Seo, E. J. Jeoung, D.-S. Suh, Y. S. Joung, I. K. Yoo, I. R. Hwang, S. H. Kim, I. S. Byun, J.-S. Kim, J. S. Choi, and B. H. Park, *Appl. Phys. Lett.*, **85**, 5655 (2004).
6. S. Zhang, S. Long, W. Guan, Q. Liu, Q. Wang, and M. Liu, *J. Phys. D: Appl. Phys.*, **42**, 055112 (2009).
7. A. Beck, J. G. Bednorz, Ch. Gerber, C. Rossel, and D. Widmer, *Appl. Phys. Lett.*, **77**, 139 (2000).
8. K. M. Kim, B. J. Choi, Y. C. Shin, S. Choi, and C. S. Huang, *Appl. Phys. Lett.*, **91**, 012907 (2007).
9. K. L. Chopra, *J. Appl. Phys.*, **36**, 184 (1965).
10. T. W. Hickmott, *J. Appl. Phys.*, **33**, 2669 (1962).
11. Q. Liu, W. Guan, S. Long, R. Jia, and M. Liu, *Appl. Phys. Lett.*, **92**, 012117 (2008).
12. H.-C. Tseng, T.-C. Chang, J.-J. Huang, P.-C. Yang, Y.-T. Chen, F.-Y. Jian, S. M. Sze, and M.-J. Tsai, *Appl. Phys. Lett.*, **99**, 132104 (2011).
13. H.-C. Tseng, T.-C. Chang, J.-J. Huang, Y.-T. Chen, P.-C. Yang, H.-C. Huang, D.-S. Gan, N.-J. Ho, S. M. Sze, and M.-J. Tsai, *Thin Solid Films*, **520**, 1656 (2011).
14. M. J. Rozenberg, I. H. Inoue, and M. J. Sánchez, *Phys. Rev. Lett.*, **92**, 178302 (2004).
15. J. F. Gibbons and W. E. Beadle, *Solid-State Electron.*, **7**, 785 (1964).
16. K. Tsunoda, Y. Fukuzumi, J. R. Jameson, Z. Wang, P. B. Griffin, and Y. Nishi, *Appl. Phys. Lett.*, **90**, 113501 (2007).
17. N. A. Tulina, S. A. Zver'kov, Y. M. Mukovskii, and D. A. Shulyatev, *Europhys. Lett.*, **56**, 836 (2001).
18. J. G. Simmons and R. R. Verderber, *Proc. R. Soc. London, Ser. A*, **301**, 77 (1967).
19. S. Q. Liu, N. J. Wu, and A. Ignatiev, *Appl. Phys. Lett.*, **76**, 2749 (2000).
20. D. Eom, S. Y. No, H. Park, C. S. Hwang, and H. J. Kim, *Electrochem. Solid-State Lett.*, **10**, G93 (2007).
21. S. Jou, B. R. Hwang, and C. J. Li, *Proceedings of the World Congress on engineering* 2011, Vol II, WCE 2011, July 6–8, 2011, London, U.K.
22. P. Zhou, M. Yin, H. J. Wan, H. B. Lu, T. A. Tang, and Y. Y. Lin, *Appl. Phys. Lett.*, **94**, 053510 (2009).
23. C. Chen, Y. C. Yang, F. Zeng, and F. Pan, *Appl. Phys. Lett.*, **97**, 083502 (2010).
24. Z. Fang, H. Y. Yu, W. J. Liu, K. L. Pey, X. Li, L. Wu, Z. R. Wang, P. G. Q. Lo, B. Gao, and J. F. Kang, *Proc. IEEE Int. Reliab. Phys. Symp.*, 964 (2010).
25. E. Cho, S. Han, H.-S. Ahn, K.-R. Lee, S. K. Kim, and C. S. Hwang, *Phys. Rev. B*, **73**, 193202 (2006).
26. D. S. Jeong, H. Schroeder, and R. Waser, *Phys. Rev. B*, **79**, 195317 (2009).
27. C. Vallee, P. Gonon, C. Jorel, and F. E. Kamel, *Appl. Phys. Lett.*, **96**, 233504 (2010).